

Formation of 8-Nitroguanine Due to Reaction between Guanyl Radical and Nitrogen Dioxide: Catalytic Role of Hydration

Neha Agnihotri and P. C. Mishra*

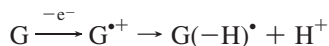
Department of Physics, Banaras Hindu University Varanasi 221 005, India

Received: December 30, 2009; Revised Manuscript Received: April 08, 2010

8-Nitroguanine (8-NitroG) is known to be a potent mutagenic product obtained from the guanine base of DNA that induces GC to AT transversion mutation. Its formation by the reaction of guanyl radical with nitrogen dioxide radical (NO_2^\bullet) has been observed experimentally. The reaction was studied here theoretically considering different reactant complexes, transition states, intermediate complexes, and product complexes. The solvent effect due to one, two, three, and six specific water molecules and the bulk solvent effect of aqueous media on the reaction were considered. With one, two, and three complexed water molecules, geometry optimization calculations were performed using the B3LYP and BHandHLYP functionals of density functional theory along with the 6-31G (d,p) and the AUG-cc-pVDZ basis sets in gas phase which was followed by single point energy calculations at the MP2/AUG-cc-pVDZ level. With six complexed water molecules, geometry optimization was performed at the BHandHLYP/6-31G(d,p) level of theory followed by single point energy calculations at all the other levels of theory mentioned above. Solvation in bulk aqueous media was treated at all the above-mentioned levels of theory using the polarizable continuum model (PCM). Specific water molecules were found to play catalytic roles in proton transfer processes that usually lowered the barrier appreciably.

1. Introduction

Harmful effects of radiation include DNA damage that may lead to aging, mutation, cancer, and various neurodegenerative diseases.^{1–5} DNA damage is mainly caused by its reaction with free radicals including the reactive oxygen species (ROS), reactive nitrogen oxide species (RNOS), high energy radiation, UV radiation, and chemicals, and by electron or hole transfer.^{6,7} Many reactions of DNA bases with ROS and RNOS result in the formation of mutagenic products.^{8–11} Interaction of DNA with high energy radiation causes ionization of the bases, with that of the guanine (G) base being most dominant due to its lowest ionization potential among all the bases.¹² The guanine radical cation ($\text{G}^{\bullet+}$) thus formed rapidly deprotonates with the rate constant 10^7 s^{-1} to produce the guanyl radical [$\text{G}(-\text{H})^\bullet$] at pH 7.¹³ This reaction can be shown as follows:



This reaction has been observed in pulse radiolysis,¹³ transient absorption spectroscopy,¹⁴ electron spin resonance (ESR),¹⁵ and X-ray photoelectron spectroscopy.¹⁶ Deprotonation of the DNA bases would be most likely to occur at the nitrogen sites, one of which in each case is also the site of a glycosidic bond in DNA.^{17,18} Different tautomers of the guanyl radical $\text{G}(-\text{H})^\bullet$ can be generated by proton transfer from the different nitrogen centers (i.e., N1, N2, and N9)¹⁹ of $\text{G}^{\bullet+}$, which can play important roles in DNA damage. These radicals are long-lived and their lifetimes have been reported from laser flash photolysis studies²⁰ to be in the range 0.2–0.6 s in oxygen-saturated solutions. These radicals are the primary targets of attack by ROS and RNOS.

The nitrogen dioxide radical (NO_2^\bullet) is an important RNOS present in biological environments.²¹ It can produce serious consequences in biological media by reacting with other radical species or closed-shell systems, particularly by abstracting hydrogen atoms.^{22–25} It can be generated by the activation of neutrophils and macrophages.²¹ In neutrophils, oxidation of nitrogen dioxide anions (NO_2^-) by H_2O_2 catalyzed by myeloperoxidase results in the formation of NO_2^\bullet .²⁶ Activation of macrophages involves the production of NO^\bullet and superoxide radicals which combine to form the toxic compound peroxynitrite.²⁷ Catalytic homolysis of peroxynitrite involving CO_2 generates NO_2^\bullet in vivo with the rate constant of $1.0 \times 10^6 \text{ s}^{-1}$.^{28–30} Free radicals including NO_2^\bullet preferentially attack the C8 site of guanine.^{31–33} NO_2^\bullet undergoes rapid reactions with the guanyl radical.¹¹ The reaction of NO_2^\bullet at the C8 site of the guanyl radical leads to the formation of 8-nitroguanine (8-NitroG).¹¹ It is potentially mutagenic because it causes rapid depurination of DNA that may lead to GC to AT transversion.^{34–36} 8-NitroG is also a potent biomarker to evaluate the risk of inflammation-associated carcinogenesis like some other modified DNA bases such as 8-oxoguanine (8-oxoGua), which is a well-known biomarker of oxidative DNA damage³⁴ and which has been named as 8-oxo-7,8-dihydroguanine in some previous studies.³⁷

The reaction of $\text{G}^{\bullet+}$ with NO_2^\bullet leading to the formation of the mutagenic product 8-NitroG^{•+} in the presence of specific water molecules was studied in detail.³⁸ Reactions of NO_2^\bullet with a single tautomer of the guanyl radical $\text{G}(-\text{H})^\bullet$ and with the corresponding tautomer of guanine radical cation have also been studied³⁹ using density functional theory. It was found that the reaction involving guanine radical cation would be more favorable than that involving the guanyl radical.³⁹ It has been found that the presence of water molecules lowers certain barrier energies significantly.³⁸ It is highly desirable to study the mechanisms of reactions of NO_2^\bullet with the different possible

* To whom correspondence should be addressed. E-mail: pc mishra_in@yahoo.com

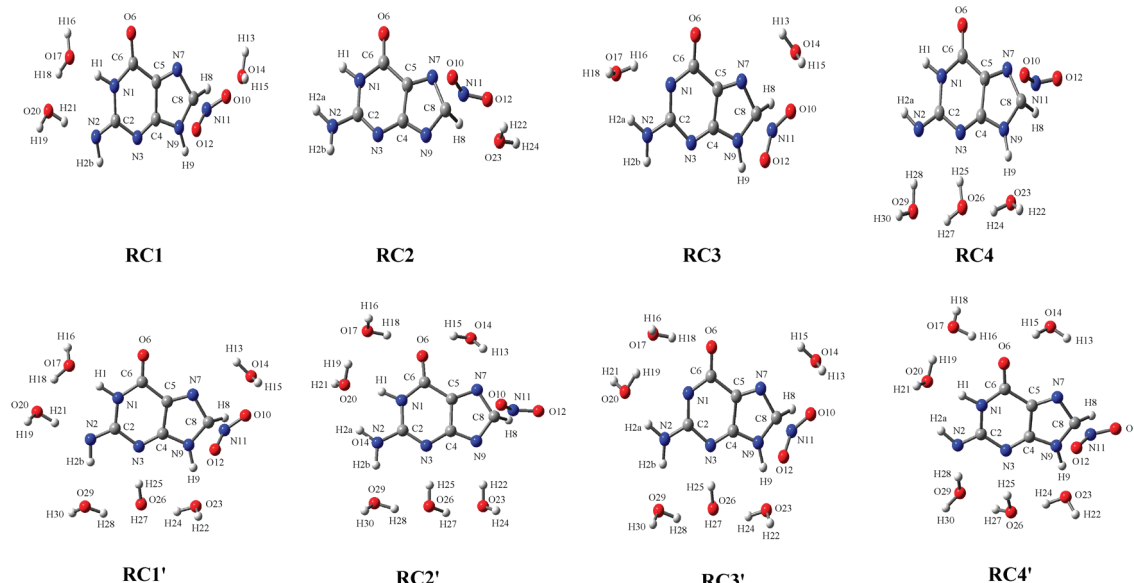


Figure 1. Structures of the reactant complexes RC1, RC2, RC3, RC4, RC1', RC2', RC3', and RC4' of the different tautomers of the guanyl radical with an NO_2^{\cdot} and one, two, three, or six water molecules obtained at the BHandHLYP/6-31G(d,p) level of theory in gas phase along with the adopted atomic numbering scheme.

tautomers of the guanyl radical considering different numbers of surrounding water molecules in detail to find out the most probable reaction mechanism, in view of seriously limited available³⁹ information in this context and its great importance with regard to mutation and cancer.^{34–36} We have carried out such a study here and have investigated the roles of surrounding specific water molecules that facilitate proton transfer involved in the reactions in detail.

2. Computational Methodology

Reactions of the guanyl radical with the nitrogen dioxide radical were studied using the three-parameter hybrid B3LYP and half-and-half BHandHLYP functionals of density functional theory (DFT)^{40,41} along with the double- ζ 6-31G(d,p) and augmented correlation consistent double- ζ AUG-cc-pVDZ basis sets. All the geometry optimization calculations on the reactions were carried out in the presence of one, two, three, or six complexed water molecules at the BHandHLYP/6-31G(d,p) level of density functional theory. The geometry optimization calculations on the reactions in the presence of one, two, or three complexed water molecules were also carried out at the B3LYP/AUG-cc-pVDZ and BHandHLYP/AUG-cc-pVDZ levels of density functional theory, which were followed by single point energy calculations at the MP2/AUG-cc-pVDZ level^{42,43} employing the geometries obtained at the BHandHLYP/AUG-cc-pVDZ level in gas phase. However, in the presence of six water molecules, geometry optimization calculations were performed only at the BHandHLYP/6-31G(d,p) level of theory in gas phase, which were followed by single point energy calculations using the BHandHLYP, B3LYP, and MP2 methods along with the AUG-cc-pVDZ basis set. Bulk solvent effect was treated for one, two, or three complexed water molecules by performing single point energy calculations at the BHandHLYP/6-31G(d,p), B3LYP/AUG-cc-pVDZ, BHandHLYP/AUG-cc-pVDZ, and MP2/AUG-cc-pVDZ levels of theory employing the geometries obtained at the respective levels in gas phase using the polarizable continuum model (PCM) of self-consistent reaction field (SCRF) theory.^{44,45} For six complexed water molecules, single point energy calculations using the PCM were performed at the BHandHLYP/6-31G(d,p), B3LYP/AUG-cc-

pVDZ, BHandHLYP/AUG-cc-pVDZ and MP2/AUG-cc-pVDZ levels of theory employing the geometries obtained at the BHandHLYP/6-31G(d,p) level in gas phase.

Vibrational frequency analysis was carried out in each geometry optimization calculation. Zero point energy (ZPE) corrections to total energy and thermal energy corrections to Gibbs free energy were made at the temperature 298.15 K. Reactant complexes (RCs), intermediate complexes (ICs), and product complexes (PCs) were characterized by all real vibrational frequencies, whereas transition states (TSs) were characterized by one imaginary vibrational frequency each. Genuineness of the optimized transition states was ensured by visually examining the vibrational mode corresponding to the imaginary frequency in each case. Intrinsic reaction coordinate (IRC) calculations⁴⁶ were not required for this purpose.

The zero point energy corrections and thermal energy corrections yielding Gibbs free energies obtained by geometry optimization calculations in gas phase, as an approximation, were also taken to be valid for the corresponding single point energy calculations in gas phase and aqueous media. Point charges located at the atomic sites were obtained at the MP2/AUG-cc-pVDZ level of theory in aqueous media by surface molecular electrostatic potential (MEP) fitting using the CHelpG algorithm.⁴⁷ All gas phase calculations were performed employing the Windows versions of the Gaussian 98 (G98W)⁴⁸ and Gaussian 03 (G03W)⁴⁹ programs, while all solvation calculations in aqueous media were performed employing the G98W program. For visualization of optimized structures and vibrational modes, the GaussView⁵⁰ program was employed.

3. Results and Discussion

Occurrence of the different tautomeric forms of the guanyl radical in DNA can lead to biologically significant consequences.^{51,52} In the present study, we have considered four different tautomers of the guanyl radical obtained by (i) removal of each of the two protons of the NH_2 group, one at a time, from guanine producing the two radicals $\text{G}(-\text{H2a})^{\cdot}$ and $\text{G}(-\text{H2b})^{\cdot}$ (the protons located nearer the N1 and N3 atoms are denoted by “a” and “b”, respectively), (ii) deprotonation of the N1 site producing the radical $\text{G}(-\text{H1})^{\cdot}$, and (iii) deprotonation of the N9 site

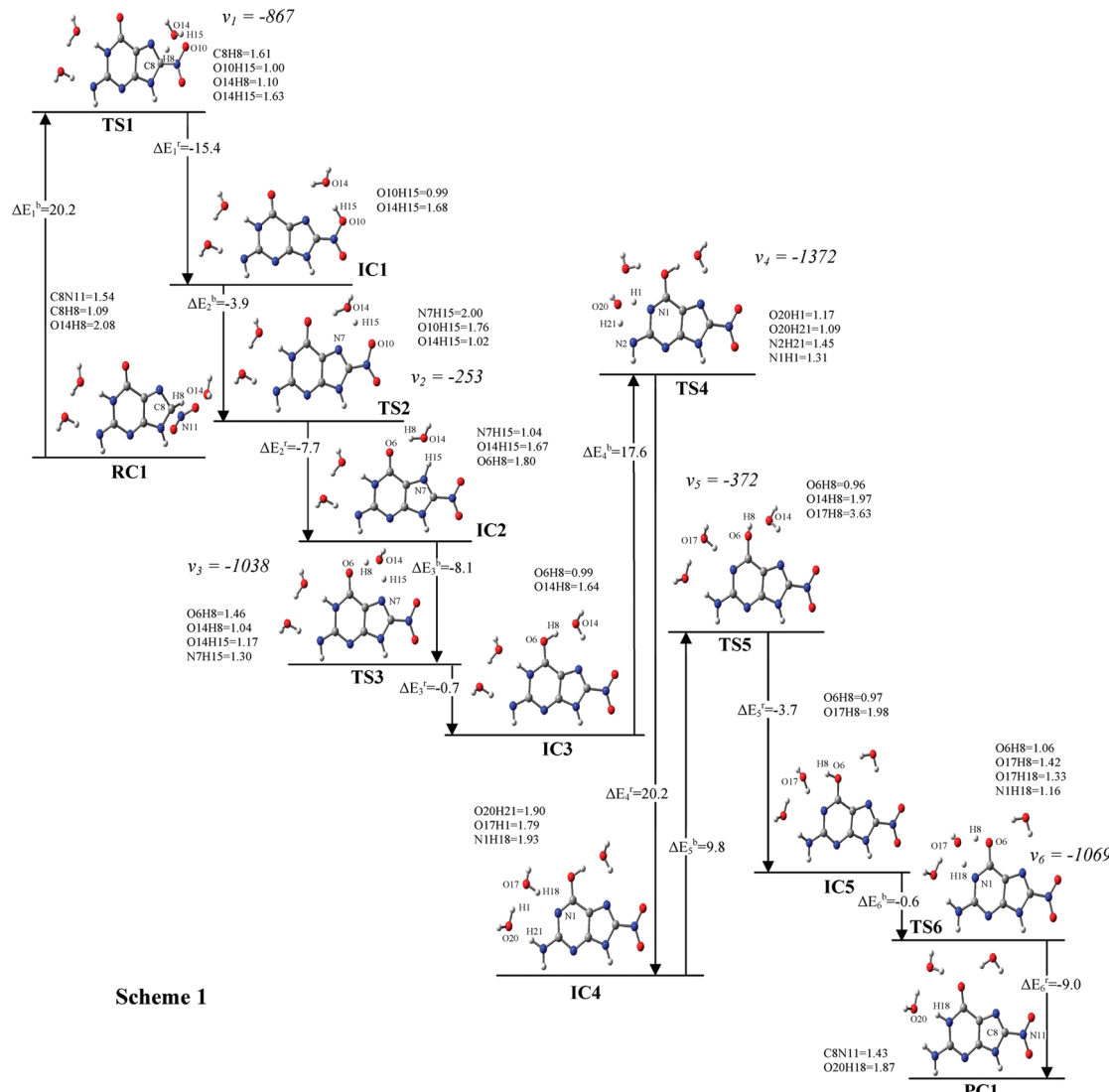


Figure 2. Reactant complex (RC1), intermediate complexes (IC1, IC2, IC3, IC4, IC5), product complex (PC1), and transition states (TS1, TS2, TS3, TS4, TS5, TS6) involved in the reaction of NO_2^{\bullet} at the C8 site of $\text{G}(-\text{H2a})^{\bullet}$ in the presence of three water molecules. ZPE-corrected barrier energies at 298.15 K (kcal/mol) obtained at the MP2/AUG-cc-pVDZ level of theory in aqueous media are given. The imaginary vibrational frequencies (ν) associated with all TSs are given in cm^{-1} .

producing the radical $\text{G}(-\text{H9})^{\bullet}$. Geometries of all four tautomers of the guanyl radical were fully optimized in gas phase using the B3LYP and BHandHLYP functionals of density functional theory along with the AUG-cc-pVDZ basis set. The relative stabilities of the four tautomers $\text{G}(-\text{H2a})^{\bullet}$, $\text{G}(-\text{H9})^{\bullet}$, $\text{G}(-\text{H1})^{\bullet}$, and $\text{G}(-\text{H2b})^{\bullet}$ at the BHandHLYP/AUG-cc-pVDZ level of theory were found to be 0.0, 2.0, 3.7, and 4.7, respectively. Thus the most stable gas phase tautomer of the guanyl radical was found to be $\text{G}(-\text{H2a})^{\bullet}$. This result is in agreement with that obtained by Schaefer and co-workers.^{53,54} However, it is reported on the basis of a DFT and electron spin resonance (ESR) study⁵⁵ that, with the involvement of seven water molecules, the most stable tautomer of the guanyl radical is $\text{G}(-\text{H1})^{\bullet}$. In the present work, reactions of NO_2^{\bullet} at the C8 sites of all four tautomers of the guanyl radical were studied. Thus there are four possible mechanisms of reactions between the guanyl radical and NO_2^{\bullet} leading to the formation of 8-NitroG. Different numbers of water molecules were allowed to participate in the reactions under study to facilitate proton transfer. In these reactions, due to formation of the $\text{C}_8-\text{NO}_2^{\bullet}$ bond, the H8 proton moves through the water molecules to the different deprotonated sites of the guanyl radical. In each of the reaction schemes 1–4 (Figures

2–5), one to three water molecules required for proton transfer were considered. In scheme 1 (Figure 2), three water molecules are required to facilitate the proton transfer from C8 to N2 via N7, O6, while in scheme 2 (Figure 3) only one water molecule is necessary to facilitate transfer of the proton from C8 to N9. Scheme 3 (Figure 4) involves two water molecules to facilitate proton transfer from C8 to N1, while in scheme 4 (Figure 5) three water molecules are required to facilitate transfer of the proton from C8 to N2 via N3. We have also studied all the above-mentioned proton transfer reactions considering the involvement of six water molecules (schemes 5–8) and found different amounts of changes in the barrier energies (Figures 6–9) obtained with the smaller numbers of water molecules mentioned above (Tables 5–8).

Eight different reactant complexes denoted by RC1, RC2, RC3, RC4, RC1', RC2', RC3', and RC4' (Figure 1) are involved in the different reaction schemes, but in each case the same stable product 8-NitroG complexed with different numbers of water molecules is formed (Figures 2–9). ZPE-corrected barrier and released energies (kcal/mol) obtained at the MP2/AUG-cc-pVDZ level of theory in aqueous media are presented in Figures 2–9. In Figures 2–5, certain optimized geometric

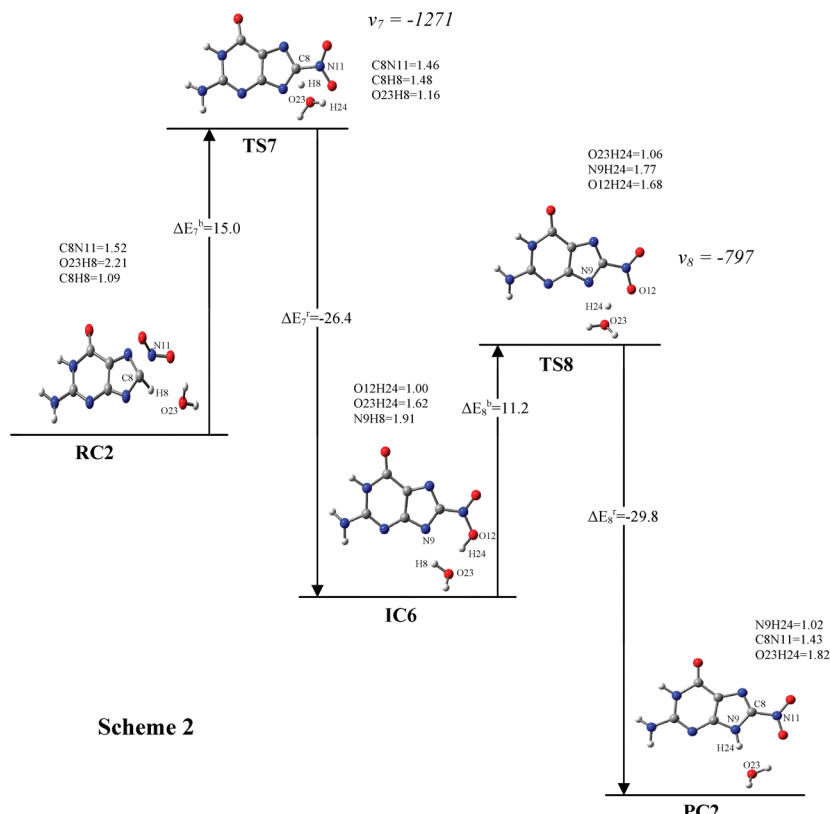


Figure 3. Reactant complex (RC2), intermediate complex (IC6), product complex (PC2), and transition states (TS7, TS8) involved in the reaction of NO_2^{\bullet} at the C8 site of $\text{G}(-\text{H9})^{\bullet}$ in the presence of a water molecule. ZPE-corrected barrier energies at 298.15 K (kcal/mol) obtained at the MP2/AUG-cc-pVDZ level of theory in aqueous media are given. The imaginary vibrational frequencies (v) associated with all TSs are given in cm^{-1} .

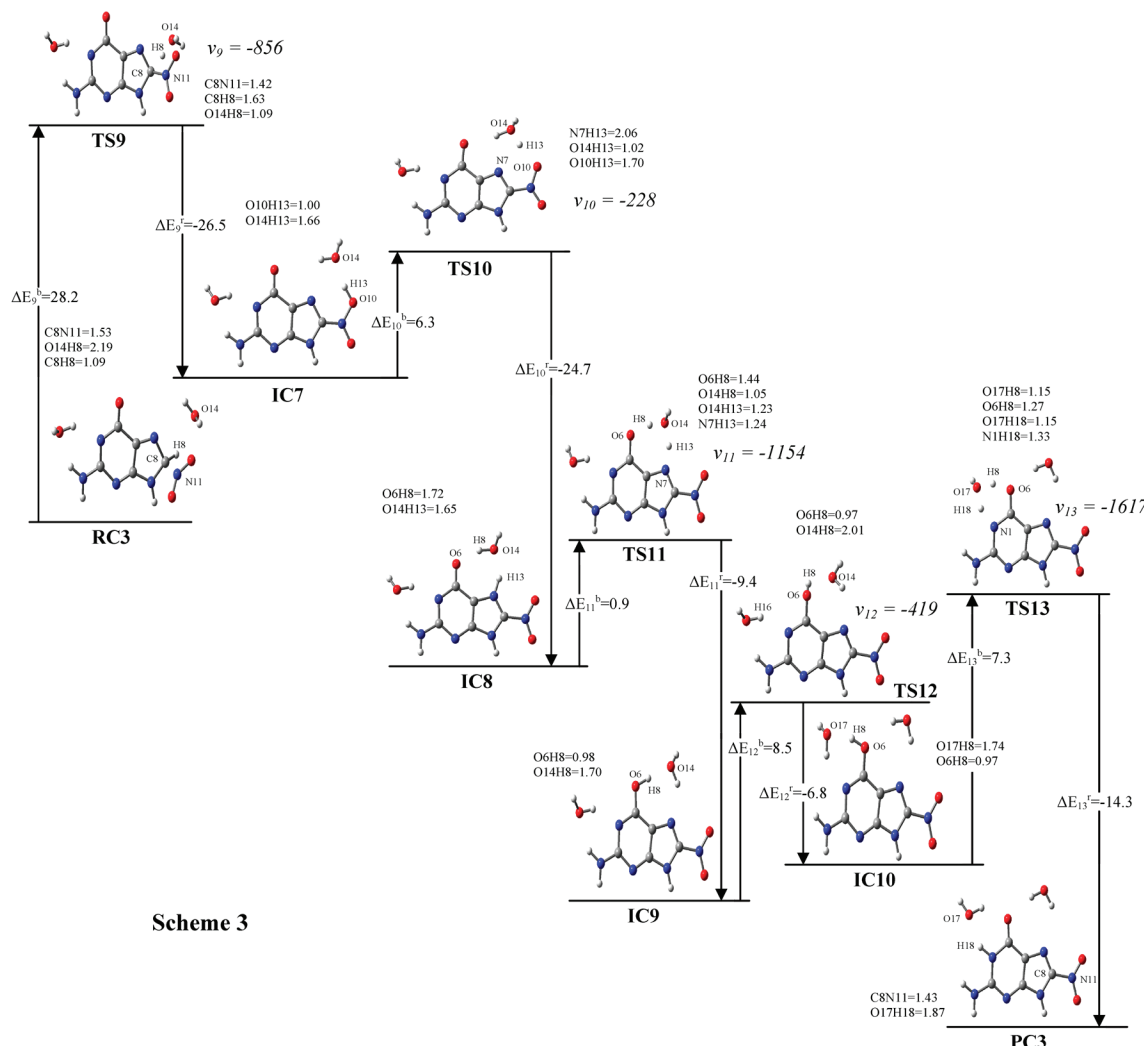
parameters of transition states, intermediates, and products involving one, two, or three complexed water molecules obtained at the BHandHLYP/AUG-cc-pVDZ level of theory in gas phase are presented, while in Figures 6–9, certain optimized geometric parameters of systems involving six water molecules each obtained at the BHandHLYP/6-31G(d,p) level of theory are presented. The calculated ZPE-corrected barrier energies and the corresponding Gibbs free energy barriers involved in the various steps of the reactions, obtained at the different levels of theory in gas phase and aqueous media, are presented in Tables 1–8. The values of the corresponding energies obtained at the different levels of theory are quite similar, their differences not exceeding 10 kcal/mol (Tables 1–8). In the following discussion, we will mainly consider these energies obtained at the MP2/AUG-cc-pVDZ level of theory in aqueous media.

3.1. Transfer of Proton from C8 to Deprotonated N2 via N7, O6. The reaction scheme shown in Figure 2 involves the reactant complex RC1, intermediate complexes IC1, IC2, IC3, IC4, and IC5, transition states TS1, TS2, TS3, TS4, TS5, and TS6, and the product complex PC1, which is a complex of 8-NitroG with three water molecules (Figure 2). In RC1, the guanyl radical $\text{G}(-\text{H2a})^{\bullet}$ is complexed with NO_2^{\bullet} and three water molecules that are placed near the C8, N1, and N2 positions (Figure 2). At TS1, the nitro group is attached to C8 and its plane is slightly away from that of the guanine ring. A visual examination of the vibrational mode corresponding to the imaginary frequency revealed that, at TS1, the H8 proton moves between the C8 and O14 atoms. At TS1, the O14H8 distance is 1.1 Å while the sum of the total CHelpG charges at H8 and the water molecule located near C8 is 0.5, which suggests that an H_3O^+ is formed transiently. The ZPE-corrected barrier energy corresponding to TS1 (ΔE_1^b) obtained at the MP2/

AUG-cc-pVDZ level of theory in aqueous media was 20.2 kcal/mol; the corresponding Gibbs free energy barrier (ΔG_1^b) was 22.9 kcal/mol. It is noted that solvation of the system in bulk aqueous media lowers the barrier energies (ΔE_1^b and ΔG_1^b) with respect to the corresponding gas phase values appreciably (Table 1).

The intermediate complex IC1 is formed following TS1, where the H15 proton of the water molecule placed near C8 moves and gets attached to the O10 atom of the NO_2 group attached to C8. The intermediate complex IC1 gets converted to another intermediate complex IC2 at the second step involving the transition state TS2. At TS2 the distances of H15 from O10, N7, and O14 are 1.76, 2.00, and 1.02 Å, respectively. Thus, at TS2 also, an H_3O^+ is formed transiently. The total net CHelpG charge at the atoms of H_2O and H15 at TS2 is 0.7, which confirms the transient formation of an H_3O^+ (Figure 2). The vibrational mode of TS2 corresponding to its imaginary frequency involves motion of the H_3O^+ moiety only. In this mode, the H_3O^+ part rotates back and forth, remaining structurally almost unchanged, such that H15 gets hydrogen bonded alternately with the N7 and O10 atoms. Thus a transient formation of H_3O^+ at TS2 facilitates proton transfer from O10 to N7 (Figure 2). The ZPE-corrected barrier energy (ΔE_2^b) and the corresponding Gibbs free energy barrier (ΔG_2^b) involved at this step of the reaction at the MP2/AUG-cc-pVDZ level of theory in aqueous media were found to be negative, i.e., -3.9 and -1.8 kcal/mol, respectively. This suggests that the reaction step involving TS2 would be barrierless.

At the third step of the reaction, IC3 is formed from IC2 through the transition state TS3. TS3 involves movement of the protons H8 and H15. While the H15 proton moves from N7 to O14, the H8 proton moves from O14 to O6 in going



Scheme 3

Figure 4. Reactant complex (RC3), intermediate complexes (IC7, IC8, IC9, IC10), product complex (PC3), and transition states (TS9, TS10, TS11, TS12, TS13) involved in the reaction of NO_2^{\bullet} at the C8 site of $\text{G}(-\text{H1})^{\bullet}$ in the presence of two water molecules. ZPE-corrected barrier energies at 298.15 K (kcal/mol) obtained at the MP2/AUG-cc-pVDZ level of theory in aqueous media are given. The imaginary vibrational frequencies (ν) associated with all TSs are given in cm^{-1} .

from IC2 to IC3 through TS3. The reaction step involving TS3 was found to be barrierless in aqueous media at all levels of theory applied here as the corresponding barrier and Gibbs free energy barriers were negative (Table 1). At the fourth step of the reaction that involves the transition state TS4 (Figure 2), catalytic roles of two water molecules hydrogen bonded to H1 and N2 are involved. The two water molecules assist proton transfer from N1 to N2 through the transition state TS4, and thus IC4 is formed from IC3. At the MP2/AUG-cc-pVDZ level of theory in aqueous media, the ZPE-corrected barrier energy (ΔE_4^b) for this double proton transfer step was found to be 17.6 kcal/mol while the corresponding Gibbs free energy barrier (ΔG_4^b) was 18.0 kcal/mol (Table 1).

The intermediate complex IC5 is formed from IC4 through the transition state TS5. The transition state TS5 was located by scanning total energy with respect to the dihedral angle N1C6O6H8. At TS5, the dihedral angle N1C6O6H8 was found to be 90° and the H8 proton moved to and fro forming anti and syn conformations of the keto form of 8-NitroG with respect to the dihedral angle alternately; the corresponding imaginary frequency was -372 cm^{-1} . At IC4, the conformation of the system with respect to the dihedral angle N1C6O6H8 is anti, while at IC5 it is syn. At the MP2/AUG-cc-pVDZ level of theory in aqueous media, the ZPE-corrected barrier energy (ΔE_5^b) and

the corresponding Gibbs free energy barrier (ΔG_5^b) corresponding to TS5 were found to be 9.8 and 8.9 kcal/mol, respectively. The intermediate complex IC5, which is the enol form of 8-NitroG, is converted through TS6 to the product PC1, which is the keto form of 8-NitroG. At TS6, double proton transfer involving one water molecule takes place. Thus at the last step of the reaction that involves TS6, keto-enol tautomerization of 8-NitroG takes place where a single water molecule plays the catalytic role. The keto tautomer, i.e., the product PC1, is more stable than the enol tautomer, i.e., IC5, by 9.6 kcal/mol. The ZPE-corrected barrier energy (ΔE_6^b) and the corresponding Gibbs free energy barrier (ΔG_6^b) for this step were found to be -0.6 and 0.8 kcal/mol respectively at the MP2/AUG-cc-pVDZ level of theory in aqueous media (Table 1).

3.2. Transfer of Proton from C8 to Deprotonated N9. Reaction scheme 2 (Figure 3) involves the reactant complex RC2, intermediate complex IC6, transition states TS7 and TS8, and the product complex PC2, which is a complex of 8-NitroG with one water molecule located near the N9 site (scheme 2). The water molecule placed near N9 catalyzes proton transfer from C8 to N9, leading to the formation of PC2. In RC2, the NO_2^{\bullet} group is located near C8 above the ring plane. At TS7, the NO_2^{\bullet} group gets bonded to C8 lying nearly in the ring plane while the H8 proton gets detached from C8. The ZPE-corrected

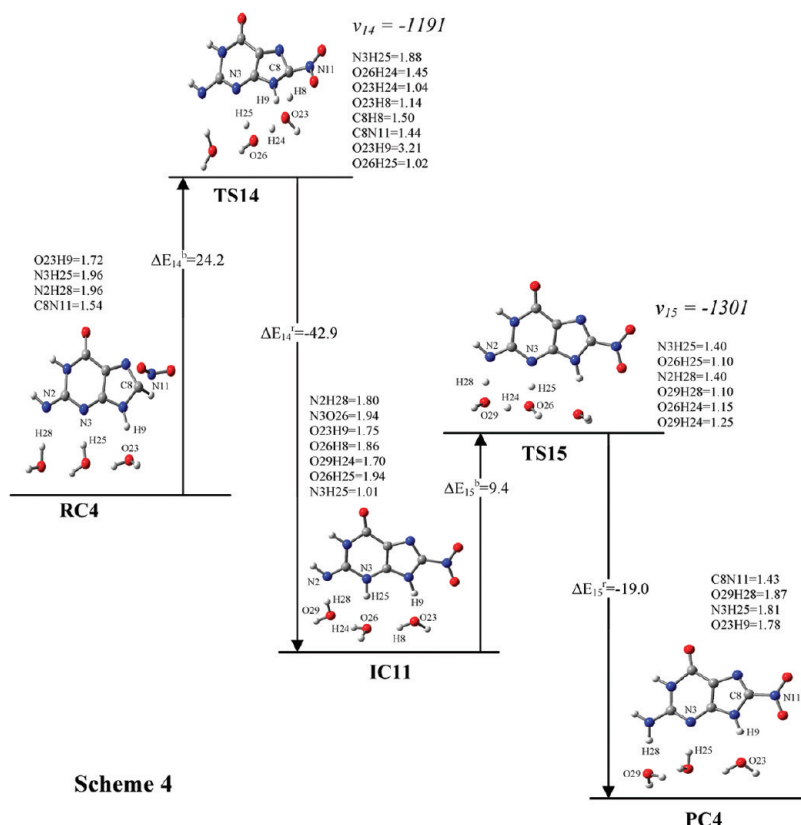
**Scheme 4**

Figure 5. Reactant complex (RC4), intermediate complex (IC11), product complex (PC4), and transition states (TS14, TS15) involved in the reaction of NO_2^* at the C8 site of G($-H_2b$) * in the presence of three water molecules. ZPE-corrected barrier energies at 298.15 K (kcal/mol) obtained at the MP2/AUG-cc-pVDZ level of theory in aqueous media are given. The imaginary vibrational frequencies (ν) associated with all TSs are given in cm^{-1} .

barrier energy ($\Delta E_7^{(b)}$) corresponding to TS7 was found to be 15.0 kcal/mol at the MP2/AUG-cc-pVDZ level of theory in aqueous media, while the corresponding Gibbs free energy ($\Delta G_7^{(b)}$) change was 18.4 kcal/mol (Table 2). The intermediate complex IC6 is formed after TS7. In IC6, the H24 proton of the water molecule located near N9 has moved and become attached to the O12 atom of the nitro group while the H8 proton has become bonded to the O23 atom of the water molecule. The product complex PC2 is formed from IC6 through TS8. At TS8, the H24 proton oscillates between N9 and O12, remaining hydrogen bonded with the O23 atom of the water molecule, and eventually gets attached to N9, producing the product complex PC2. Thus the water molecule catalyzes the proton transfer from C8 to N9. The ZPE-corrected barrier energy ($\Delta E_8^{(b)}$) involved at this step of the reaction obtained at MP2/AUG-cc-pVDZ level of theory in aqueous media was found to be 11.2 kcal/mol; the corresponding Gibbs free energy ($\Delta G_8^{(b)}$) change was 11.6 kcal/mol.

3.3. Transfer of Proton from C8 to Deprotonated N1. Reaction scheme 3 (Figure 4) involves the reactant complex RC3, intermediate complexes IC7, IC8, IC9, and IC10, transition states TS9, TS10, TS11, TS12, and TS13, and the product complex PC3, which is a complex of 8-nitroG with two water molecules. In RC3, the guanyl radical G($-H_1$) * is complexed with NO_2^* and two water molecules located near the C8 and N1 positions, with the NO_2^* group being located near C8 above the ring plane. In going from RC3 to TS9, the NO_2^* group gets bonded to C8 lying nearly in the ring plane while the H8 proton leaves C8 and gets bonded to the water molecule located near this site (Figure 4). At TS9, the total CHelpG charge on the water molecule and the attached proton H8 is 0.5, which suggests that an H_3O^+ is formed transiently. The ZPE-corrected

barrier energy ($\Delta E_9^{(b)}$) involved at this step of the reaction obtained at the MP2/AUG-cc-pVDZ level of theory in aqueous media was found to be 28.2 kcal/mol; the corresponding Gibbs free energy barrier ($\Delta G_9^{(b)}$) was 30.9 kcal/mol.

The intermediate complex IC7 is formed from TS9, where the H13 proton of the water molecule placed near C8 has moved and has become attached to the O10 atom of the NO_2 group attached to C8. IC7 gets converted to IC8 through the transition state TS10. At TS10, the H13 proton has moved from O10 and has become attached to the O14 atom of the water molecule located near N7. The total net CHelpG charge at the atoms of H_2O and H13 at TS10 is 0.7, which indicates formation of an H_3O^+ (Figure 4). At TS10, the H_3O^+ moiety rotates back and forth, remaining structurally unchanged, as revealed by the vibrational mode belonging to the corresponding imaginary vibrational frequency. Thus the transient formation of H_3O^+ at TS10 facilitates proton transfer from O10 to N7 (Figure 4). The ZPE-corrected barrier energy ($\Delta E_{10}^{(b)}$) and the corresponding Gibbs free energy barrier ($\Delta G_{10}^{(b)}$) were found to be 6.3 and 7.6 kcal/mol at the MP2/AUG-cc-pVDZ level of theory in aqueous media, respectively. The intermediate complex IC8 is formed when the system relaxes from TS10. IC9 is formed from IC8 through the transition state TS11. At TS11, while the H13 proton moves from N7 to O14 of the water molecule located near it, the H8 proton moves from O14 to O6. The ZPE-corrected barrier energy ($\Delta E_{11}^{(b)}$) involved at this double proton transfer step of the reaction at the MP2/AUG-cc-pVDZ level of theory in aqueous media was found to be 0.9 kcal/mol, while the corresponding Gibbs free energy barrier ($\Delta G_{11}^{(b)}$) was 1.6 kcal/mol (Table 3).

The intermediate complex IC10 is formed from IC9 through the transition state TS12. At TS12, the dihedral angle N1C6O6H8

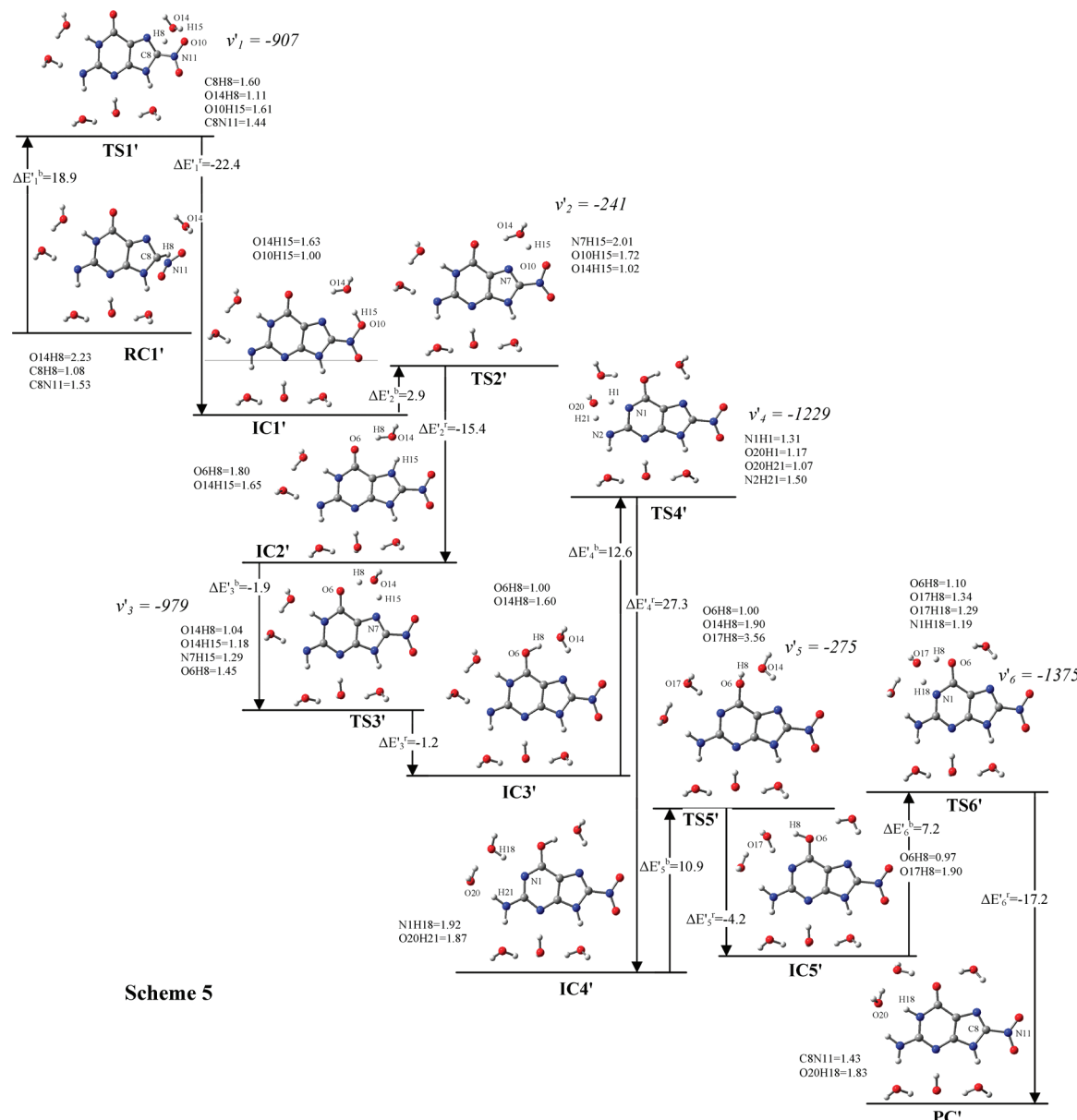


Figure 6. Reactant complex (RC1'), intermediate complexes (IC1', IC2', IC3', IC4', IC5'), product complex (PC'), and transition states (TS1', TS2', TS3', TS4', TS5', TS6') involved in the reaction of NO_2^* at the C8 site of $\text{G}(-\text{H2a})^*$ in the presence of six water molecules. ZPE-corrected barrier energies at 298.15 K (kcal/mol) obtained at the MP2/AUG-cc-pVDZ level of theory in aqueous media are given. The imaginary vibrational frequencies (ν) associated with all TSs are given in cm^{-1} .

is 90° and the H8 proton moves to and fro, forming anti and syn conformations of the keto form of 8-NitroG with respect to the dihedral angle N1C6O6H8, as revealed by the vibrational mode of the corresponding imaginary frequency. At IC9, the conformation of the system with respect to the dihedral angle N1C6O6H8 is anti, while at IC10 it is syn. The ZPE-corrected barrier energy (ΔE_{12}^b) involved in going from the anti to the syn conformation was found to be 8.5 kcal/mol while the corresponding Gibbs free energy barrier (ΔG_{12}^b) was 7.7 kcal/mol at the MP2/AUG-cc-pVDZ level of theory in aqueous media. In going from IC10 to the product complex PC3 through the transition state TS13, the water molecule placed near N1 and O6 catalyzes keto-enol tautomerism of 8-NitroG. Thus PC3 is the keto form of 8-NitroG while IC10 is the corresponding enol form of the same. PC3 is more stable than IC10 by 7 kcal/mol. The ZPE-corrected barrier energy (ΔE_{13}^b) and the corresponding Gibbs free energy barrier (ΔG_{13}^b) at the MP2/AUG-cc-pVDZ level of theory in aqueous media at the last step of

the reaction involving TS13 were found to be 7.3 and 8.7 kcal/mol, respectively (Table 3).

3.4. Transfer of Proton from C8 to Deprotonated N2 via N3. Reaction scheme 4 shown in Figure 5 involves reactant complex RC4, intermediate complex IC11, transition states TS14 and TS15, and product complex PC4, which is a complex of 8-NitroG with three water molecules placed near the H9, N3, and N2 atoms. In going from RC4 to TS14, the H8 proton gets detached from the C8 site and moves toward the water molecule located near H9 while the NO_2^* group gets bonded to C8. At this step of the reaction, the two water molecules located near H9 and N3 sites are involved in a triple proton transfer mechanism. When the H8 proton moves from C8 toward O23 of the water molecule located near H9, the H24 proton moves from O23 toward O26 of the water molecule located near N3 while the H25 proton of the latter water molecule moves from O26 toward the N3 atom. Thus at IC11, effectively, the H8 proton has moved from C8 to the N3 site. The ZPE-corrected

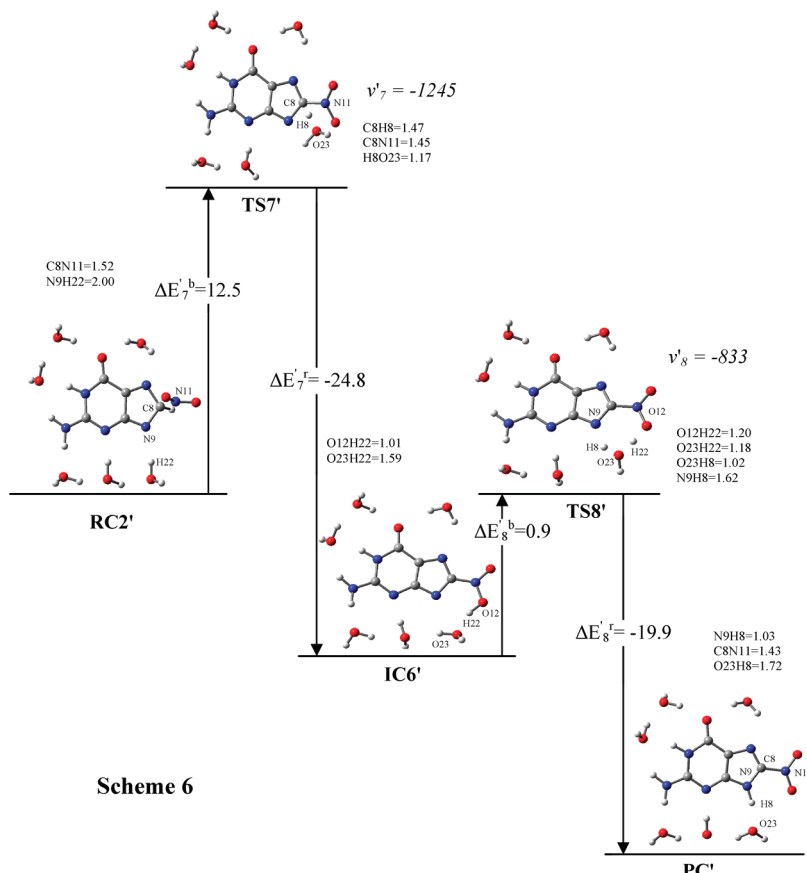


Figure 7. Reactant complex (RC2'), intermediate complex (IC6'), product complex (PC'), and transition states (TS7', TS8') involved in the reaction of NO_2^{\bullet} at the C8 site of $\text{G}(-\text{H9})^{\bullet}$ in the presence of six water molecules. ZPE-corrected barrier energies at 298.15 K (kcal/mol) obtained at the MP2/AUG-cc-pVDZ level of theory in aqueous media are given. The imaginary vibrational frequencies (ν) associated with all TSs are given in cm^{-1} .

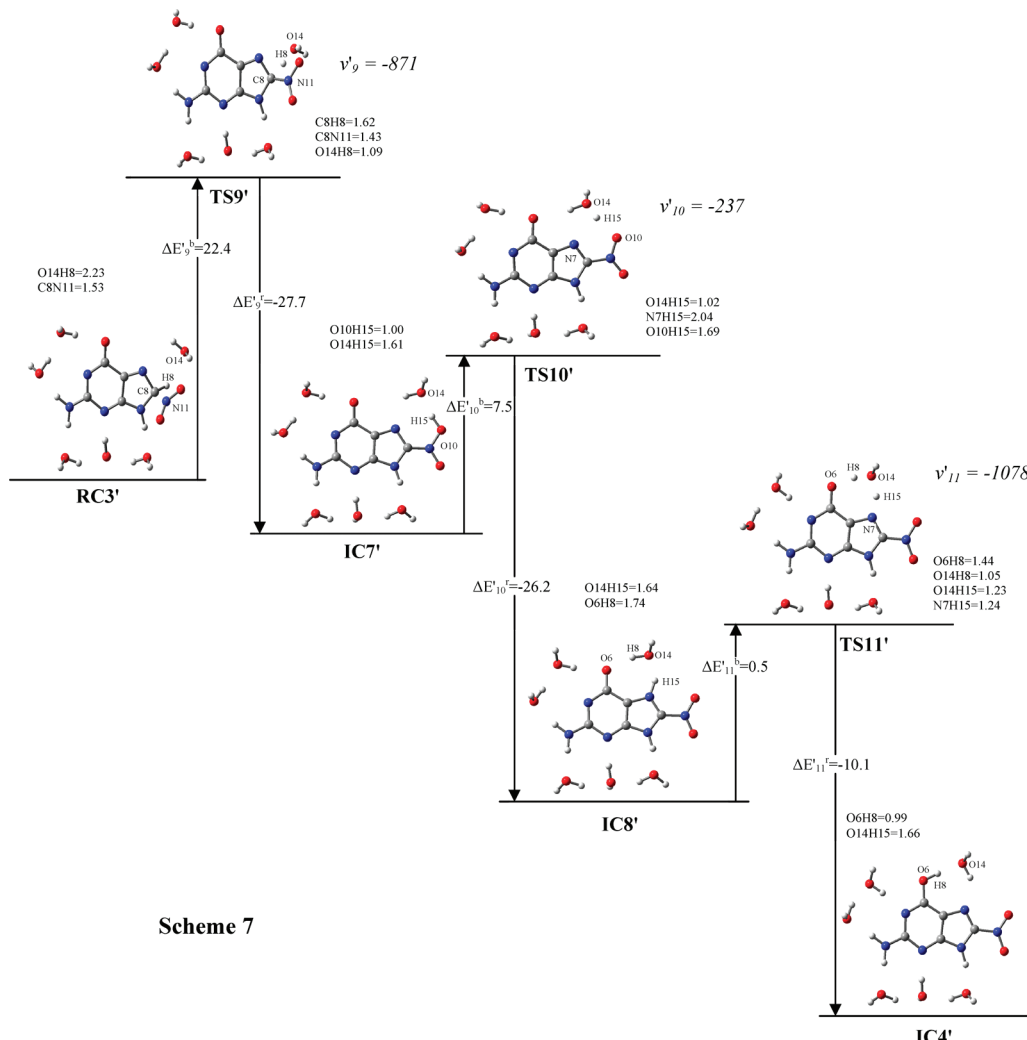
barrier energy (ΔE_{14}^b) and the corresponding Gibbs free energy barriers (ΔG_{14}^b) involved at this step of the reaction at the MP2/AUG-cc-pVDZ level of theory in aqueous media were found to be 24.2 and 27.3 kcal/mol, respectively (Table 4).

Starting from the intermediate complex IC11, the product complex PC4, which is a complex of 8-NitroG with three water molecules, is formed through the transition state TS15. At TS15 also, a triple proton transfer mechanism is operative involving two water molecules placed near the N3 and N2 sites. At this step of the reaction, the H25 proton moves from N3 toward the water molecule placed near this site while the H24 proton of this water molecule moves toward O29 of the water molecule placed near N2 and the H28 proton of the latter water molecule moves toward the N2 atom. Thus finally, PC4 is formed involving the catalytic action of the three water molecules. The ZPE-corrected barrier energy (ΔE_{15}^b) involved at the second step of the reaction obtained at the MP2/AUG-cc-pVDZ level of theory in aqueous media was found to be 9.4 kcal/mol while the corresponding Gibbs free energy barrier (ΔG_{15}^b) was 10.2 kcal/mol (Table 4).

3.5. Effects of Hydration Shell. It would be appropriate to consider a larger number of water molecules representing approximately the first hydration shell around the guanyl radical than only one, two, or three, to obtain more accurate results. Therefore, we considered six water molecules and reinvestigated the reaction mechanisms shown in Figures 2–5 (schemes 1–4). The results thus obtained are presented in Figures 6–9 (schemes 5–8). The reactant complexes involving six water molecules are denoted by RC1', RC2', RC3', and RC4' (Figures 6–9).

Reaction scheme 5 (Figure 6) involves reactant complex RC1', intermediate complexes IC1', IC2', IC3', IC4', and IC5', transition states TS1', TS2', TS3', TS4', TS5', and TS6', and product complex PC'. The reaction schemes shown in Figures 2 and 6 are similar except that, in the latter case (Figure 6), there are three additional hydrogen bonded water molecules located near the H9, N3, and H2b atoms. At the first step of this reaction, the nitro group is attached to C8 and its plane at TS1' is slightly away from that of the guanine rings. A visual inspection of the vibrational mode corresponding to the imaginary frequency related to TS1' revealed that, at TS1', the H8 proton moves between the C8 and O14 atoms similar to what is found at TS1 in scheme 1. The barrier energy ΔE_1^b and the Gibbs free energy barrier ΔG_1^b of scheme 1 (Figure 2) would correspond to the barrier energy $\Delta E'_1$ and the Gibbs free energy barrier $\Delta G'_1$ of scheme 5 (Figure 6), respectively. Although the water molecules located near the H9, N3, and H2b atoms are not directly involved in the reaction, their hydrogen bonding with these atoms changes the barrier energy significantly. The ZPE-corrected barrier energy ΔE_1^b (Figure 2) having the value 20.2 kcal/mol corresponds to the barrier energy $\Delta E'_1$ (Figure 6) having the value 18.9 kcal/mol; the corresponding Gibbs free energy barriers ΔG_1^b and $\Delta G'_1$ are 22.9 and 21.5 kcal/mol, respectively (Table 5).

Hydrogen bonding of the three additional water molecules with H9, N3, and H2b changes the second barrier energy (ΔE_2^b) of scheme 1 from -3.9 to 2.9 kcal/mol ($\Delta E'_2$) of scheme 6; the corresponding Gibbs free energy barriers ΔG_2^b and $\Delta G'_2$ are -1.8 and 3.7 kcal/mol, respectively, as obtained at the MP2/



Scheme 7

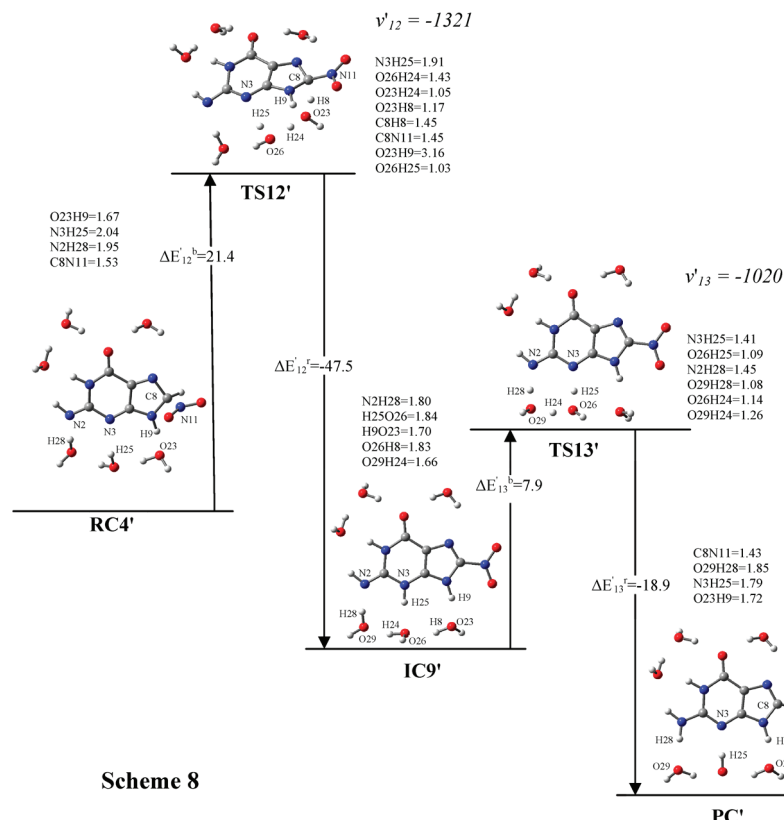
Figure 8. Reactant complex ($\text{RC3}'$), intermediate complexes ($\text{IC4}'$, $\text{IC7}'$, $\text{IC8}'$), and transition states ($\text{TS9}'$, $\text{TS10}'$, $\text{TS11}'$) involved in the reaction of NO_2^+ at the C8 site of $\text{G}(-\text{H1})^*$ in the presence of six water molecules. ZPE-corrected barrier energies at 298.15 K (kcal/mol) obtained at the MP2/AUG-cc-pVDZ level of theory in aqueous media are given. The imaginary vibrational frequencies (ν) associated with all TSs are given in cm^{-1} .

AUG-cc-pVDZ level of theory in aqueous media (Tables 1 and 5). Though at the third step of the reaction the barrier energy is increased by about 6 kcal/mol in going from three to six water molecules, in both cases (Figures 2 and 6) this reaction step is barrierless. The fourth barrier energy of the reaction gets reduced from 17.6 kcal/mol (ΔE_4^{b} , Figure 2) to 10.7 kcal/mol ($\Delta E'_4^{\text{b}}$, Figure 6), while the corresponding Gibbs free energy barrier is reduced from 18.0 to 11.2 kcal/mol in going from three to six complexed water molecules. At the fifth step of this reaction, at the MP2/AUG-cc-pVDZ level of theory in aqueous media, the ZPE-corrected barrier energy (ΔE_5^{b} , Figure 2) is increased from 9.8 to 10.9 kcal/mol ($\Delta E'_5^{\text{b}}$, Figure 6); the corresponding Gibbs free energy barriers are 8.9 and 10.4 kcal/mol, respectively (Tables 1 and 5). There is a large change in barrier energy at the sixth step of the reaction in going from three to six water molecules. Thus the sixth barrier energy (ΔE_6^{b} , Figure 2) increases from -0.6 to 7.2 kcal/mol ($\Delta E'_6^{\text{b}}$, Figure 6) while the Gibbs free energy barrier increases from 0.8 to 8.8 kcal/mol at the MP2/AUG-cc-pVDZ level of theory in aqueous media.

Reaction scheme 6 presented in Figure 7 involves the reactant complex $\text{RC2}'$, intermediate complex $\text{IC6}'$, transition states $\text{TS7}'$ and $\text{TS8}'$, and the product complex PC' . The schemes of Figures 3 and 7 are similar except that, in the latter case, there are five

additional hydrogen bonded water molecules located near the N7, O6, N1, H2b, and N3 atoms. The barrier energy ΔE_7^{b} and the Gibbs free energy barrier ΔG_7^{b} of scheme 2 (Figure 3) correspond to the barrier energy $\Delta E'_7^{\text{b}}$ and the Gibbs free energy barrier $\Delta G'_7^{\text{b}}$ of scheme 6 (Figure 7), respectively. The ZPE-corrected barrier energy (ΔE_7^{b}) of Figure 3 is reduced from 15.0 to 12.5 kcal/mol ($\Delta E'_7^{\text{b}}$, Figure 7) in going from one to six complexed water molecules; the corresponding Gibbs free energy barriers are 18.4 kcal/mol (ΔG_7^{b}) and 12.8 kcal/mol ($\Delta G'_7^{\text{b}}$), respectively (Tables 2 and 6).

In scheme 6 (Figure 7), the product complex PC' is obtained from $\text{IC6}'$ through the transition state $\text{TS8}'$, where a different water-assisted proton transfer mechanism is found to operate from that at the corresponding transition state TS8 given in Figure 3. At $\text{TS8}'$, the H22 proton is nearly equally shared by the O12 atom of the NO_2^+ group and the O23 atom of the water molecule placed near the N9 site. Further, at the transition state $\text{TS8}'$, the H8 proton of the water molecule is ready to leave the O23 atom, to move toward the N9 atom. From $\text{TS8}'$, the final product PC' , which is the complex of 8-NitroG with six water molecules, is formed. The ZPE-corrected barrier energy and the corresponding Gibbs free energy change as obtained at the MP2/AUG-cc-pVDZ level of theory in aqueous media are drastically reduced in going from scheme 2 (Figure 3) to scheme 6 (Figure



Scheme 8

Figure 9. Reactant complex (RC4'), intermediate complex (IC9'), product complex (PC'), and transition states (TS12', TS13') involved in the reaction of NO_2^\bullet at the C8 site of $\text{G}(-\text{H}2\text{b})^\bullet$ in the presence of six water molecules. ZPE-corrected barrier energies at 298.15 K (kcal/mol) obtained at the MP2/AUG-cc-pVDZ level of theory in aqueous media are given. The imaginary vibrational frequencies (ν) associated with all TSs are given in cm^{-1} .

TABLE 1: ZPE-Corrected Barrier Energies (ΔE_i^b) and Corresponding Gibbs Free Energy Barriers (ΔG_i^b) ($i = 1-6$) at 298.15 K (kcal/mol) Involved in the Reaction of NO_2^\bullet with $\text{G}(-\text{H}2\text{a})^\bullet$ in the Presence of Three Water Molecules Placed Near the C8, N1, and N2 Atoms, According to Scheme 1 in Gas Phase and Aqueous Media^a

ZPE-corrected barrier energies and corresponding Gibbs free energy changes	B3LYP/ AUG-cc-pVDZ	BHandHLYP/ 6-31G(d,p)	BHandHLYP/ AUG-cc-pVDZ	MP2/AUG-cc-pVDZ ^b
ΔE_1^b	28.4 (17.3)	31.7 (20.8)	36.7 (26.3)	31.6 (20.2)
ΔG_1^b	32.2 (21.1)	34.7 (24.1)	39.4 (29.0)	36.1 (22.9)
ΔE_2^b	18.6 (0.2)	16.6 (1.6)	19.7 (1.2)	15.1 (-3.9)
ΔG_2^b	19.6 (1.2)	17.5 (2.5)	21.8 (3.3)	17.2 (-1.8)
ΔE_3^b	1.6 (-7.1)	0.9 (-6.1)	2.7 (-6.4)	2.2 (-8.1)
ΔG_3^b	2.5 (-6.3)	1.6 (-5.4)	3.6 (-5.4)	3.2 (-7.1)
ΔE_4^b	11.0 (17.1)	12.9 (15.6)	13.6 (16.2)	8.5 (17.6)
ΔG_4^b	10.9 (17.0)	13.4 (16.1)	14.0 (16.6)	8.9 (18.0)
ΔE_5^b	11.7 (10.6)	11.5 (10.8)	10.9 (9.6)	10.5 (9.8)
ΔG_5^b	10.7 (9.6)	11.1 (10.4)	10.0 (8.6)	9.6 (8.9)
ΔE_6^b	6.3 (7.8)	8.8 (10.6)	9.7 (6.8)	7.4 (-0.6)
ΔG_6^b	7.8 (9.3)	10.6 (12.3)	11.1 (8.3)	8.8 (0.8)

^a The results obtained in aqueous media are given in parentheses. ^b Gas phase single point energy calculations were performed employing the geometries obtained at the BHandHLYP/AUG-cc-pVDZ level of theory.

7) from 11.2 (ΔE_8^b) and 11.6 (ΔG_8^b) kcal/mol to 0.9 ($\Delta E_8'$) and 1.2 ($\Delta G_8'$) kcal/mol respectively due to increase in the number of water molecules from one to six (Tables 2 and 6).

Reaction scheme 7 (Figure 8) involves the reactant complex RC3', intermediate complexes IC7', IC8', and IC4', and transition states TS9', TS10', and TS11'. Reaction schemes 3 and 7 (Figures 4 and 8) are similar except that, in the latter case, there are four additional hydrogen bonded water molecules located near the H2a, H2b, N3, and N9 sites. The barrier energy ΔE_9^b and the corresponding Gibbs free energy barrier ΔG_9^b of scheme 3 (Figure 4) correspond to the barrier energy ΔE_9^b and the Gibbs free energy barrier ΔG_9^b of scheme 7 (Figure 8), respectively.

While at the MP2/AUG-cc-pVDZ level in aqueous media the ZPE-corrected barrier energy ΔE_9^b (Figure 4) had the value 28.2 kcal/mol in the presence of two water molecules, the corresponding barrier energy in the presence of six water molecules ($\Delta E_9'^b$) had the value 22.4 kcal/mol (Figure 8), and the corresponding Gibbs free energy barriers were 30.9 (ΔG_9^b) and 24.8 kcal/mol ($\Delta G_9'^b$), respectively (Tables 3 and 7).

However, in the same situation, as obtained at the MP2/AUG-cc-pVDZ level of theory in aqueous media (Tables 3 and 7), the second barrier energy (ΔE_{10}^b , Figure 4) is increased from 6.3 to 7.5 kcal/mol ($\Delta E_{10}'^b$, Figure 8); the corresponding Gibbs free energy barriers are 7.6 and 8.3 kcal/mol, respectively. At

TABLE 2: ZPE-Corrected Barrier Energies (ΔE_i^b) and Corresponding Gibbs Free Energy Barriers (ΔG_i^b) ($i = 7, 8$) at 298.15 K (kcal/mol) Involved in the Reaction of NO_2^* with $\text{G}(-\text{H9})^*$ in the Presence of a Water Molecule Placed Near the N9 Atom, According to Scheme 2 in Gas Phase and Aqueous Media^a

ZPE-corrected barrier energies and corresponding Gibbs free energy changes	B3LYP/ AUG-cc-pVDZ	BHandHLYP/ 6-31G(d,p)	BHandHLYP/ AUG-cc-pVDZ	MP2/AUG-cc-pVDZ ^b
ΔE_7^b	21.0 (20.9)	23.7 (16.4)	26.6 (25.3)	18.7 (15.0)
ΔG_7^b	24.0 (23.9)	26.1 (18.9)	30.0 (28.7)	22.1 (18.4)
ΔE_8^b	19.6 (13.4)	18.6 (-3.2)	18.8 (17.0)	17.4 (11.2)
ΔG_8^b	19.9 (13.7)	19.0 (-2.8)	19.2 (17.4)	17.7 (11.6)

^a The results obtained in aqueous media are given in parentheses. ^b Gas phase single point energy calculations were performed employing the geometries obtained at the BHandHLYP/AUG-cc-pVDZ level of theory.

TABLE 3: ZPE-Corrected Barrier Energies (ΔE_i^b) and Corresponding Gibbs Free Energy Barriers (ΔG_i^b) ($i = 9–13$) at 298.15 K (kcal/mol) Involved in the Reaction of NO_2^* with $\text{G}(-\text{H1})^*$ in the Presence of Two Water Molecules Placed Near the C8 and N1 Atoms, According to Scheme 3 in Gas Phase and Aqueous Media^a

ZPE-corrected barrier energies and corresponding Gibbs free energy changes	B3LYP/ AUG-cc-pVDZ	BHandHLYP/ 6-31G(d,p)	BHandHLYP/ AUG-cc-pVDZ	MP2/AUG-cc-pVDZ ^b
ΔE_9^b	27.4 (25.9)	33.6 (27.1)	38.1 (33.2)	34.5 (28.2)
ΔG_9^b	31.9 (30.4)	36.2 (29.7)	40.7 (35.8)	37.2 (30.9)
ΔE_{10}^b	14.9 (13.5)	12.5 (8.4)	15.9 (13.0)	10.7 (6.3)
ΔG_{10}^b	15.8 (14.4)	13.5 (9.4)	17.2 (14.3)	12.0 (7.6)
ΔE_{11}^b	-0.3 (0.9)	-0.7 (1.1)	0.6 (2.2)	-0.3 (0.9)
ΔG_{11}^b	0.3 (1.5)	-0.2 (1.6)	1.3 (3.1)	0.4 (1.6)
ΔE_{12}^b	12.0 (8.5)	12.1 (11.1)	11.2 (8.1)	10.9 (8.5)
ΔG_{12}^b	10.8 (7.3)	11.5 (10.5)	10.4 (7.3)	10.1 (7.7)
ΔE_{13}^b	7.9 (7.3)	10.4 (9.4)	11.7 (10.7)	8.4 (7.3)
ΔG_{13}^b	9.2 (8.6)	11.6 (10.6)	13.1 (12.1)	9.8 (8.7)

^a The results obtained in aqueous media are given in parentheses. ^b Gas phase single point energy calculations were performed employing the geometries obtained at the BHandHLYP/AUG-cc-pVDZ level of theory.

TABLE 4: ZPE-Corrected Barrier Energies (ΔE_i^b) and Corresponding Gibbs Free Energy Barriers (ΔG_i^b) ($i = 14, 15$) at 298.15 K (kcal/mol) Involved in the Reaction of NO_2^* with $\text{G}(-\text{H2b})^*$ in the Presence of Three Water Molecules Placed Near the H9, N3, and N2 Atoms, According to Scheme 4 in Gas Phase and Aqueous Media^a

ZPE-corrected barrier energies and corresponding Gibbs free energy changes	B3LYP/ AUG-cc-pVDZ	BHandHLYP/ 6-31G(d,p)	BHandHLYP/ AUG-cc-pVDZ	MP2/AUG-cc-pVDZ ^b
ΔE_{14}^b	24.8 (20.7)	18.1 (18.0)	29.8 (22.6)	29.3 (24.2)
ΔG_{14}^b	27.4 (23.3)	21.3 (21.3)	32.5 (25.3)	32.0 (27.3)
ΔE_{15}^b	5.5 (8.1)	11.9 (11.4)	14.3 (13.4)	10.7 (9.4)
ΔG_{15}^b	7.0 (9.7)	12.5 (12.0)	15.2 (14.3)	11.6 (10.2)

^a The results obtained in aqueous media are given in parentheses. ^b Gas phase single point energy calculations performed employing the geometries obtained at the BHandHLYP/AUG-cc-pVDZ level of theory.

the third step of the reaction, there is only a slight change in the barrier energy in going from two to six complexed water molecules. Thus while at this step, at the MP2/AUG-cc-pVDZ level of theory, the ZPE-corrected barrier energy (ΔE_{11}^b , Figure 4) decreases from 0.9 to 0.5 kcal/mol ($\Delta E'_{11}^b$, Figure 8), the corresponding Gibbs free energy barrier increases from 1.6 to 1.7 kcal/mol. At the third step of the reaction in scheme 7, the intermediate complex IC4' is formed from where the reaction proceeds in the same way as shown in scheme 5 after formation of the corresponding complex (not shown in scheme 7), leading to the final product PC' (Figure 6). The fourth step of the reaction scheme 7 (not shown) is similar to the fifth step of the reaction shown in scheme 5 where the intermediate complex IC5' is formed through the transition state TS5'. Thus in scheme 7 also the final product complex PC' is formed through the transition state TS6'.

Reaction scheme 8 (Figure 9) involves the reactant complex RC4', intermediate complex IC9', transition states TS12' and TS13', and the product complex PC'. Schemes 4 and 8 (Figures 5 and 9) are similar except that, in the latter case, there are three additional hydrogen bonded water molecules located near

the N7, O6, and N1 sites. In going from RC4' to TS12', the H8 proton gets detached from the C8 site and moves toward the water molecule located near H9 while the NO_2^* group gets bonded to C8. At TS12', the two water molecules located near the H9 and N3 sites are involved in a triple proton transfer mechanism. When the H8 proton moves from C8 toward O23 of the water molecule located near H9, the H24 proton moves from O23 toward O26 of the water molecule located near N3 while the H25 proton of the latter water molecule moves from O26 toward the N3 atom. Thus in going from RC4' to IC9', effectively, the H8 proton has moved from the C8 to the N3 site. This reaction step is similar to the one that involves TS14 in scheme 4. The barrier energy ΔE_{14}^b and the Gibbs free energy barrier ΔG_{14}^b of scheme 4 (Figure 5) correspond to the barrier energy $\Delta E'_{12}^b$ and the Gibbs free energy barrier $\Delta G'_{12}^b$ of scheme 8 (Figure 9), respectively. The ZPE-corrected barrier energy ΔE_{14}^b of scheme 4 (Figure 5) is reduced from 24.2 to 21.4 kcal/mol ($\Delta E'_{12}^b$, Figure 9) in going from three to six complexed water molecules, while the corresponding Gibbs free energy barriers in the two schemes are from 27.3 (ΔG_{14}^b) and 40.0 kcal/mol ($\Delta G'_{12}^b$) respectively (Table 8). Similarly, the

TABLE 5: ZPE-Corrected Barrier Energies ($\Delta E'_i{}^b$) and Corresponding Gibbs Free Energy Barriers ($\Delta G'_i{}^b$) ($i = 1\text{--}6$) at 298.15 K (kcal/mol) Involved in the Reaction of NO_2^\bullet with $\text{G}(-\text{H}2\text{a})^\bullet$ in the Presence of Six Water Molecules Placed Near the C8, N1, N2, H2b, N3, and H9 Atoms, According to Scheme 5 in Gas Phase and Aqueous Media^a

ZPE-corrected barrier energies and corresponding Gibbs free energy changes	B3LYP/ AUG-cc-pVDZ ^b	BHandHLYP/ 6-31G(d,p)	BHandHLYP/ AUG-cc-pVDZ ^b	MP2/ AUG-cc-pVDZ ^b
$\Delta E'_1{}^b$	26.8 (18.6)	31.1 (23.1)	32.7 (30.0)	29.0 (18.9)
$\Delta G'_1{}^b$	29.4 (22.8)	33.7 (25.7)	35.2 (27.6)	31.6 (21.5)
$\Delta E'_2{}^b$	18.0 (6.4)	16.1 (5.1)	18.4 (6.1)	15.4 (2.9)
$\Delta G'_2{}^b$	18.9 (7.3)	17.0 (6.0)	19.3 (7.0)	16.3 (3.7)
$\Delta E'_3{}^b$	2.2 (-1.6)	1.8 (-2.0)	3.3 (-0.4)	2.9 (-1.9)
$\Delta G'_3{}^b$	2.9 (-0.9)	2.5 (-1.3)	4.0 (0.3)	3.6 (-1.2)
$\Delta E'_4{}^b$	12.0 (13.2)	12.9 (14.2)	14.4 (15.7)	9.6 (10.7)
$\Delta G'_4{}^b$	12.5 (13.7)	13.3 (14.7)	14.9 (16.2)	10.1 (11.2)
$\Delta E'_5{}^b$	12.1 (11.0)	12.1 (11.1)	11.4 (10.4)	11.1 (10.9)
$\Delta G'_5{}^b$	11.7 (10.6)	11.7 (10.7)	11.0 (9.9)	10.7 (10.4)
$\Delta E'_6{}^b$	6.1 (7.8)	8.5 (10.3)	9.5 (11.2)	6.6 (7.2)
$\Delta G'_6{}^b$	7.8 (9.4)	10.2 (11.9)	11.1 (12.8)	8.2 (8.8)

^a The results obtained in aqueous media are given in parentheses. ^b Gas phase single point energy calculations performed employing the geometries obtained at the BHandHLYP/6-31G(d,p) level of theory.

TABLE 6: ZPE-Corrected Barrier Energies ($\Delta E'_i{}^b$) and Corresponding Gibbs Free Energy Barriers ($\Delta G'_i{}^b$) ($i = 7, 8$) at 298.15 K (kcal/mol) Involved in the Reaction of NO_2^\bullet with $\text{G}(-\text{H}9)^\bullet$ in the Presence of Six Water Molecules Placed Near the C8, N1, N2, H2b, N3, and H9 Atoms, According to Scheme 6 in Gas Phase and Aqueous Media^a

ZPE-corrected barrier energies and corresponding Gibbs free energy changes	B3LYP/ AUG-cc-pVDZ ^b	BHandHLYP/ 6-31G(d,p)	BHandHLYP/ AUG-cc-pVDZ ^b	MP2/ AUG-cc-pVDZ ^b
$\Delta E'_7{}^b$	23.8 (15.1)	27.9 (17.1)	28.7 (21.0)	21.7 (12.5)
$\Delta G'_7{}^b$	24.1 (15.5)	28.3 (17.5)	29.1 (21.4)	22.0 (12.8)
$\Delta E'_8{}^b$	0.1 (-0.9)	1.2 (0.0)	1.6 (0.6)	1.6 (0.9)
$\Delta G'_8{}^b$	0.4 (-0.6)	1.5 (0.3)	1.9 (0.9)	1.9 (1.2)

^a The results obtained in aqueous media are given in parentheses. ^b Gas phase single point energy calculations performed employing the geometries obtained at the BHandHLYP/6-31G(d,p) level of theory.

TABLE 7: ZPE-Corrected Barrier Energies ($\Delta E'_i{}^b$) and Corresponding Gibbs Free Energy Barriers ($\Delta G'_i{}^b$) ($i = 5, 6, 9\text{--}11$) at 298.15 K (kcal/mol) Involved in the Reaction of NO_2^\bullet with $\text{G}(\text{H}1)^\bullet$ in the Presence of Six Water Molecules Placed Near the C8, N1, N2, H2b, N3, and H9 Atoms, According to Scheme 7 in Gas Phase and Aqueous Media^a

ZPE-corrected barrier energies and corresponding Gibbs free energy changes	B3LYP/ AUG-cc-pVDZ ^b	BHandHLYP/ 6-31G(d,p)	BHandHLYP/ AUG-cc-pVDZ ^b	MP2/AUG-cc-pVDZ ^b
$\Delta E'_9{}^b$	28.5 (20.1)	33.8 (25.9)	34.7 (26.8)	0.8 (22.4)
$\Delta G'_9{}^b$	30.9 (22.5)	36.2 (28.3)	7.0 (29.2)	33.2 (24.8)
$\Delta E'_{10}{}^b$	16.0 (8.3)	13.1 (9.0)	15.7 (12.5)	11.7 (7.5)
$\Delta G'_{10}{}^b$	16.8 (9.0)	13.8 (9.7)	16.4 (13.3)	12.5 (8.3)
$\Delta E'_{11}{}^b$	-1.6 (0.1)	-1.7 (0.5)	-0.2 (1.8)	-0.9 (0.5)
$\Delta G'_{11}{}^b$	-0.5 (1.2)	-0.6 (1.6)	0.9 (2.9)	0.2 (1.7)
$\Delta E'_5{}^b$	12.1 (11.0)	12.1 (11.1)	11.4 (10.4)	11.1 (10.9)
$\Delta G'_5{}^b$	11.7 (10.6)	11.7 (10.7)	11.0 (9.9)	10.7 (10.4)
$\Delta E'_6{}^b$	6.1 (7.8)	8.5 (10.3)	9.5 (11.2)	6.6 (7.2)
$\Delta G'_6{}^b$	7.8 (9.4)	10.2 (11.9)	11.1 (12.8)	8.2 (8.8)

^a The results obtained in aqueous media are given in parentheses. ^b Gas phase single point energy calculations performed employing the geometries obtained at the BHandHLYP/6-31G(d,p) level of theory.

ZPE-corrected barrier energy $\Delta E_{14}{}^b$ of scheme 4 (Figure 5) gets reduced from 9.4 to 7.9 kcal/mol ($\Delta E'_{12}{}^b$, Figure 9); the corresponding Gibbs free energy barriers are 10.2 and 8.5 kcal/mol, respectively (Table 8).

The results discussed above show that certain proton transfer barrier energies are modified significantly while other barrier energies are changed only mildly in going from one, two, or three to six complexed water molecules. Certain reaction steps that were barrierless with one, two, or three water molecules have acquired small barrier energies with six water molecules. However, the overall qualitative features of the reactions remain unchanged in going from one, two, or three to six complexed water molecules.

We note that 2'-deoxyguanosine would be more relevant to the DNA environment than guanine. The radical ($\text{G}(-\text{R}9)^\bullet$, R = sugar moiety) can also be formed by cleavage of the glycosidic bond of 2'-deoxyguanosine,^{56–58} and the present results would correspond to that situation. However, if the glycosidic bond is not cleaved, the next most favored radical for attack of the NO_2^\bullet group leading to the formation of 8-NitroG would be $\text{G}(-\text{H}2\text{b})^\bullet$, though the barrier energies are substantially higher in the case of $\text{G}(-\text{H}2\text{b})^\bullet$ than those in the case of $\text{G}(-\text{H}9)^\bullet$ (Tables 6 and 8).

Surfaces of the molecular electrostatic potential (MEP) of RC2', TS7', IC6', TS8', and PC' of scheme 6 for the 0.5 kcal/mol value of MEP are shown in parts a, b, c, d, and e,

TABLE 8: ZPE-Corrected Barrier Energies ($\Delta E'_{i^b}$) and Corresponding Gibbs Free Energy Barriers ($\Delta G'_{i^b}$) ($i = 12, 13$) at 298.15 K (kcal/mol) Involved in the Reaction of NO_2^{\bullet} with $\text{G}(-\text{H}2\text{b})^{\bullet}$ in the Presence of Six Water Molecules Placed near the C8, N1, N2, H2b, N3, and H9 Atoms, According to Scheme 8 in Gas Phase and Aqueous Media^a

ZPE-corrected barrier energies and corresponding Gibbs free energy changes	B3LYP/AUG-cc-pVDZ ^b	BHandHLYP/6-31G(d,p)	BHandHLYP/AUG-cc-pVDZ ^b	MP2/AUG-cc-pVDZ ^b
$\Delta E'_{12}^b$	23.7 (22.5)	25.5 (24.1)	28.1 (28.1)	23.1 (21.4)
$\Delta G'_{12}^b$	26.3 (25.1)	28.1 (26.7)	30.7 (30.7)	25.7 (24.0)
$\Delta E'_{13}^b$	10.1 (7.6)	11.6 (10.0)	14.0 (11.5)	11.1 (7.9)
$\Delta G'_{13}^b$	10.6 (8.2)	12.1 (10.5)	14.5 (12.0)	11.6 (8.5)

^a The results obtained in aqueous media are given in parentheses. ^b Gas phase single point energy calculations performed employing the geometries obtained at BHandHLYP/6-31G(d,p) level of theory.

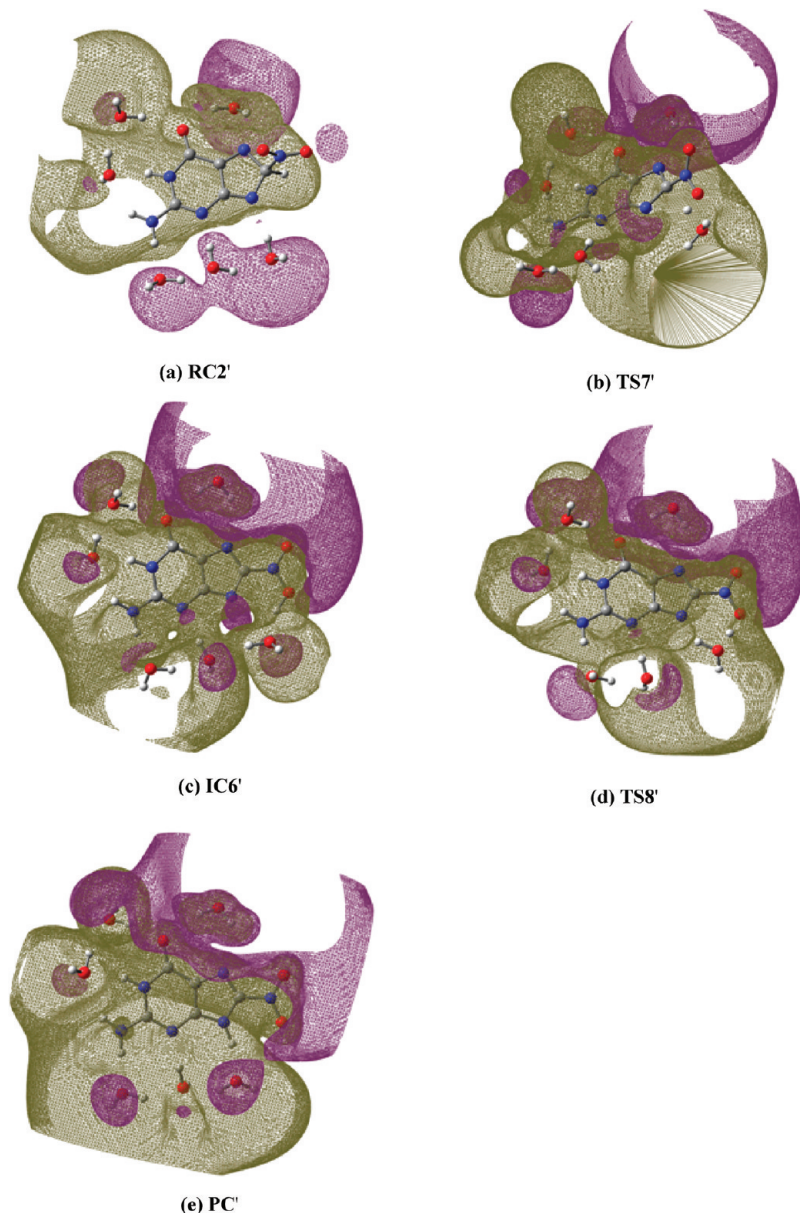


Figure 10. Molecular electrostatic potential (MEP) surfaces (a–e) of the reactant complex $\text{RC2}'$, transition states $\text{TS7}'$ and $\text{TS8}'$, intermediate complex $\text{IC6}'$, and product complex PC' involved in the reaction between $\text{G}(-\text{H}9)^{\bullet}$ and NO_2^{\bullet} shown in scheme 6 (Figure 7) obtained at the MP2/AUG-cc-pVDZ level of theory in aqueous media. The surfaces shown in (a)–(e) correspond to 0.5 kcal/mol.

respectively, of Figure 10. This reaction scheme was selected since it appears to be most favorable on the basis of the calculated Gibbs free energy barriers. Generally, negative MEP regions are found to be located near the oxygen atoms of the water molecules in these maps. However, it is not true near the oxygen atom O23 at the transition states $\text{TS7}'$ and $\text{TS8}'$ which

is involved in proton transfer. We can examine the charge distributions approximately in terms of electrostatic potential derived point charges. We considered (CHelpG) point charges here.⁴⁷ The point charge at H8 in $\text{TS7}'$ is 0.15, while the total charge at H8 and the water molecule located nearby is 0.45. The charge at H22 in $\text{TS8}'$ is 0.48, while the total charge at

H22 and the water molecule located near it is 0.67. Thus the water molecules located near H8 and H22 at TS7' and TS8' respectively carry significant positive charges. This explains why O23 is not associated with negative MEP regions at TS7' and TS8'.

4. Conclusions

We arrive at the following conclusions from the present study:

1. Explicit inclusion of water molecules in the proton transfer reactions between the guanyl radical and NO_2^\bullet reduces many barrier energies drastically. In these reactions, the water molecules act as catalysts.

2. The first barrier energy corresponding to bonding between NO_2^\bullet and the guanyl radical at the C8 site of the latter, accompanied by detachment of the H8 proton from this site, is found to be largest among the different barrier energies in each reaction scheme. However, the barrier energy for this reaction step is lowest for the G(-H9) $^\bullet$ tautomer of the guanyl radical among the barrier energies of the corresponding reaction occurring in the different tautomers. Therefore, the proton transfer from C8 to deprotonated N9 would be most preferred. In the case of 2'-deoxyguanosine, the radical corresponding to G(-H9) $^\bullet$ of guanine would be G(-R9) $^\bullet$ (R = sugar moiety), which would be formed by cleavage of the glycosidic bond. The Gibbs free energy barriers at both the first and second steps of this reaction with six complexed water molecules were found to be 12.8 and 1.2 kcal/mol, respectively. Thus it appears that this reaction would occur fairly rapidly.

Acknowledgment. The authors are thankful to the University Grants Commission (New Delhi) and the Council of Scientific and Industrial Research (New Delhi) for financial support.

References and Notes

- (1) Collins, G. P. *Sci. Am.* **2003**, 289, 26.
- (2) Ames, B. N. *Free Radical Res. Commun.* **1989**, 7, 121.
- (3) Mecocci, P.; Macgarvey, U.; Beal, M. F. *J. J. Neurochem.* **1998**, 71, 2034.
- (4) von Sonntag, C. *The chemical basis of radiation biology*; Taylor and Francis: London, 1987.
- (5) Mishra, S. K.; Mishra, P. C. *Int. J. Quantum Chem.* **1979**, 16, 1051.
- (6) Burrows, C. J.; Muller, J. G. *Chem. Rev.* **1998**, 98, 1109.
- (7) Cadet, J.; Douki, T.; Gasparutto, D.; Ravanat, J. L. *Mutat. Res.* **2003**, 531, 5.
- (8) Liu, R. H.; Hotchkiss, J. H. *Mutat. Res.* **1995**, 339, 73.
- (9) Wiseman, H.; Halliwell, B. *Biochem. J.* **1996**, 313, 17.
- (10) Niles, J. C.; Wishnok, J. S.; Tannenbaum, S. R. *Nitric Oxide* **2006**, 14, 109.
- (11) Misiaszek, R.; Crean, C.; Geacintov, N. E.; Shafirovich, V. *J. Am. Chem. Soc.* **2005**, 127, 2191.
- (12) Steenken, S. *Chem. Rev.* **1989**, 89, 503.
- (13) Kobayashi, K.; Tagawa, S. *J. Am. Chem. Soc.* **2003**, 125, 10213.
- (14) Shafirovich, V.; Dourandin, A.; Huang, W.; Geacintov, N. E. *J. Biol. Chem.* **2001**, 276, 24621.
- (15) Schiemann, O.; Turro, N. J.; Barton, J. K. *J. Phys. Chem. B* **2000**, 104, 7214.
- (16) Furukawa, M.; Kato, H. S.; Taniguchi, M.; Kawai, T.; Hatsui, T.; Kosugi, N.; Yoshida, T.; Aida, M.; Kawai, M. *Phys. Rev. B* **2007**, 75, 045119.
- (17) Lind, M. C.; Bera, P. P.; Richardson, N. A.; Wheeler, S. E.; Schaefer, H. F., III. *Proc. Natl. Acad. Sci. U.S.A.* **2006**, 103, 7554.
- (18) Abdoul-Carime, H.; Gohlke, S.; Illenberger, E. *Phys. Rev. Lett.* **2004**, 92, 168103.
- (19) Jena, N. R.; Mishra, P. C.; Suhai, S. *J. Phys. Chem. B* **2009**, 113, 5633.
- (20) Misiaszek, R.; Crean, C.; Joffe, A.; Geacintov, N. E.; Shafirovich, V. *J. Biol. Chem.* **2004**, 279, 32106.
- (21) Dedon, P. C.; Tannenbaum, S. R. *Arch. Biochem. Biophys.* **2004**, 423, 12.
- (22) Augusto, O.; Bonini, M. G.; Amanso, A. M.; Linares, E.; Santos, C. C. X.; De Menezes, S. L. *Free Radical Biol. Med.* **2002**, 32, 841.
- (23) Prutz, W. A.; Monig, H.; Butler, J.; Land, E. *J. Arch. Biochem. Biophys.* **1985**, 243, 125.
- (24) Alfassi, Z. B.; Huie, R. E.; Neta, P. *J. Phys. Chem.* **1986**, 90, 4156.
- (25) Titov, A. I. *Tetrahedron* **1979**, 19, 557.
- (26) Burner, U.; Furtmuller, P. G.; Kettle, A. J.; Koppenol, W. H.; Obinger, C. *J. Biol. Chem.* **2000**, 275, 20587.
- (27) Beckman, J. S.; Beckman, T. W.; Chen, J.; Marshall, P. A.; Freeman, B. A. *Proc. Natl. Acad. Sci. U.S.A.* **1990**, 87, 1620.
- (28) Ischiropoulos, H.; Beckman, J. S. *J. Clin. Invest.* **2003**, 111, 163.
- (29) Davis, K. L.; Martin, E.; Turko, I. V.; Murad, F. *Annu. Rev. Pharmacol. Toxicol.* **2001**, 41, 203.
- (30) Pryor, W. A.; Lemercier, J. N.; Zhang, H.; Uppu, R. M.; Squadrato, G. L. *Free Radical Biol. Med.* **1997**, 23, 331.
- (31) Jena, N. R.; Mishra, P. C. *J. Comput. Chem.* **2007**, 28, 1321.
- (32) Shukla, P. K.; Mishra, P. C. *J. Phys. Chem. B* **2008**, 112, 4779.
- (33) Jena, N. R.; Mishra, P. C. *J. Phys. Chem. B* **2005**, 109, 14205.
- (34) Yermilov, V.; Rubio, J.; Ohshima, H. *FEBS Lett.* **1995**, 376, 207.
- (35) Suzuki, N.; Yasui, M.; Geacintov, N. E.; Shafirovich, V.; Shibutani, S. *Biochemistry* **2005**, 44, 9238.
- (36) Kaneko, K.; Akuta, T.; Sawa, T.; Kim, H. W.; Fujii, S.; Okamoto, T.; Nakayama, H.; Ohigashi, H.; Murakami, A.; Akaite, T. *Cancer Lett.* **2008**, 262, 239.
- (37) Cadet, J.; Douki, T.; Ravanat, J. L. *Acc. Chem. Res.* **2008**, 41, 1075.
- (38) Agnihotri, N.; Mishra, P. C. *J. Phys. Chem. B* **2009**, 113, 3129.
- (39) Liu, N.; Ban, F.; Boyd, R. J. *J. Phys. Chem. A* **2006**, 110, 9908.
- (40) Becke, A. D. *J. Chem. Phys.* **1993**, 98, 5648.
- (41) Lee, C.; Yang, W.; Parr, R. G. *Phys. Rev. B* **1988**, 37, 785.
- (42) Frisch, M. J.; Head-Gordon, M.; Pople, J. A. *Chem. Phys. Lett.* **1990**, 166, 275.
- (43) Møller, C.; Plesset, M. S. *Phys. Rev.* **1934**, 46, 618.
- (44) Miertus, S.; Tomasi, J. *Chem. Phys.* **1982**, 65, 239.
- (45) Miertus, S.; Scrocco, E.; Tomasi, J. *Chem. Phys.* **1981**, 55, 117.
- (46) Gonzalez, C.; Schlegel, H. B. *J. Chem. Phys.* **1989**, 90, 2154.
- (47) Breneman, C. M.; Wiberg, K. B. *J. Comput. Chem.* **1990**, 11, 361.
- (48) Frisch, M. J.; Trucks, G. W.; Schlegel, H. B.; Scuseria, G. E.; Robb, M. A.; Cheeseman, J. R.; Zakrzewski, V. G.; Montgomery, J. A., Jr.; Stratmann, R. E.; Burant, J. C.; Dapprich, S.; Millam, J. M.; Daniels, A. D.; Kudin, K. N.; Strain, M. C.; Farkas, O.; Tomasi, J.; Barone, V.; Cossi, M.; Cammy, R.; Mennucci, B.; Pomelli, C.; Adamo, C.; Clifford, S.; Ochterski, J.; Petersson, G. A.; Ayala, P. Y.; Cui, Q.; Morokuma, K.; Rega, N.; Salvador, P.; Dannenberg, J. J.; Malick, D. K.; Rabuck, A. D.; Raghavachari, K.; Foresman, J. B.; Cioslowski, J.; Ortiz, J. V.; Baboul, A. G.; Stefanov, B. B.; Liu, G.; Liashenko, A.; Piskorz, P.; Komaromi, I.; Comperts, R.; Martin, R. L.; Fox, D. J.; Keith, T.; Al-Laham, M. A.; Peng, C. Y.; Nanayakkara, A.; Challacombe, M.; Gill, P. M. W.; Johnson, B.; Chen, W.; Wong, M. W.; Andres, J. L.; Gonzalez, C.; Head-Gordon, M.; Replogle, E. S.; Pople, J. A. *Gaussian 98*, revision A.11.2; Gaussian, Inc.: Pittsburgh, PA, 2001.
- (49) Frisch, M. J.; Trucks, G. W.; Schlegel, H. B.; Scuseria, G. E.; Robb, M. A.; Cheeseman, J. R.; Montgomery, J. A., Jr.; Vreven, T.; Kudin, K. N.; Burant, J. C.; Millam, J. M.; Iyengar, S. S.; Tomasi, J.; Barone, V.; Mennucci, B.; Cossi, M.; Scalmani, G.; Rega, N.; Petersson, G. A.; Nakatsuji, H.; Hada, M.; Ehara, M.; Toyota, K.; Fukuda, R.; Hasegawa, J.; Ishida, M.; Nakajima, T.; Honda, Y.; Kitao, O.; Nakai, H.; Klene, M.; Li, X.; Knox, J. E.; Hratchian, H. P.; Cross, J. B.; Bakken, V.; Adamo, C.; Jaramillo, J.; Gomperts, R.; Stratmann, R. E.; Yazyev, O.; Austin, A. J.; Cammi, R.; Pomelli, C.; Ochterski, J. W.; Ayala, P. Y.; Morokuma, K.; Voth, G. A.; Salvador, P.; Dannenberg, J. J.; Zakrzewski, V. G.; Dapprich, S.; Daniels, A. D.; Strain, M. C.; Farkas, O.; Malick, D. K.; Rabuck, A. D.; Raghavachari, K.; Foresman, J. B.; Ortiz, J. V.; Cui, Q.; Baboul, A. G.; Clifford, S.; Cioslowski, J.; Stefanov, B. B.; Liu, G.; Liashenko, A.; Piskorz, P.; Komaromi, I.; Martin, R. L.; Fox, D. J.; Keith, T.; Al-Laham, M. A.; Peng, C. Y.; Nanayakkara, A.; Challacombe, M.; Gill, P. M. W.; Johnson, B.; Chen, W.; Wong, M. W.; Gonzalez, C.; Pople, J. A. *Gaussian 03*, revision D.01; Gaussian, Inc.: Wallingford, CT, 2004.
- (50) Frisch, A. E.; Dennington, R. D.; Keith, T. A.; Neilsen, A. B.; Holder, A. J. *GaussView*, revision 3.9; Gaussian, Inc.: Pittsburgh, PA, 2003.
- (51) Hole, E. O.; Sagstuen, E.; Nelson, W. H.; Close, D. M. *Radiat. Res.* **1992**, 129, 119.
- (52) Hole, E. O.; Sagstuen, E.; Nelson, W. H.; Close, D. M. *Radiat. Res.* **1991**, 125, 119.
- (53) Luo, Q.; Li, Q. S.; Xie, Y.; Schaefer, H. F., III. *Collect. Czech. Chem. Commun.* **2005**, 70, 826.
- (54) Bera, P. P.; Schaefer, H. F., III. *Proc. Natl. Acad. Sci. U.S.A.* **2005**, 102, 6698.
- (55) Adhikary, A.; Kumar, A.; Becker, D.; Sevilla, M. D. *J. Phys. Chem. B* **2006**, 110, 24171.
- (56) Mishra, S. K.; Mishra, P. C. *J. Comput. Chem.* **2002**, 23, 530.
- (57) Shim, E. J.; Przybylski, J. L.; Wetmore, S. D. *J. Phys. Chem. B* **2010**, 114, 2319.
- (58) Rios-Font, R.; Rodriguez-Santiago, L.; Bertran, J.; Sodupe, M. J. *Phys. Chem. B* **2007**, 111, 6071.